The Plant Cell, Vol. 22: 2417–2428, July 2010, www.plantcell.org

Spatial Uncoupling of Mitosis and Cytokinesis during Appressorium-Mediated Plant Infection by the Rice Blast Fungus *Magnaporthe oryzae* [W]

Diane G.O. Saunders,[1] Yasin F. Dagdas, and Nicholas J. Talbot[2]

School of Biosciences, University of Exeter, Exeter EX4 4QD, United Kingdom

To infect plants, many pathogenic fungi develop specialized infection structures called appressoria. Here, we report that appressorium development in the rice blast fungus *Magnaporthe oryzae* involves an unusual cell division, in which nuclear division is spatially uncoupled from the site of cytokinesis and septum formation. The position of the appressorium septum is defined prior to mitosis by formation of a heteromeric septin ring complex, which was visualized by spatial localization of Septin4:green fluorescent protein (GFP) and Septin5:GFP fusion proteins. Mitosis in the fungal germ tube is followed by long-distance nuclear migration and rapid formation of an actomyosin contractile ring in the neck of the developing appressorium, at a position previously marked by the septin complex. By contrast, mutants impaired in appressorium development, such as Δ*pmk1* and Δ*cpkA* regulatory mutants, undergo coupled mitosis and cytokinesis within the germ tube. Perturbation of the spatial control of septation, by conditional mutation of the *SEPTATION-ASSOCIATED1* gene of *M. oryzae*, prevented the fungus from causing rice blast disease. Overexpression of *SEP1* did not affect septation during appressorium formation, but instead led to decoupling of nuclear division and cytokinesis in nongerminated conidial cells. When considered together, these results indicate that *SEP1* is essential for determining the position and frequency of cell division sites in *M. oryzae* and demonstrate that differentiation of appressoria requires a cytokinetic event that is distinct from cell divisions within hyphae.

INTRODUCTION

The position and orientation of cell division is pivotal in the development of multicellular organisms (Oliferenko et al., 2009). Although cell division can often lead to daughter cells of equal size, in many instances, cells of unequal size and fate are generated. The differentiation of new cell types, tissues, and organs, for example, requires distinct patterns of cell division in which the machinery that physically divides a cell is subject to precisely synchronized genetic regulation (Oliferenko et al., 2009). In pathogenic fungi, which are responsible for some of the most serious plant diseases, the ability to cause disease relies on the ability to form specialized cells, such as spores and infection structures (Tucker and Talbot, 2001). The genetic regulation of cell division in these organisms is, however, not well understood, especially during infection-associated development (Tucker and Talbot, 2001; Gladfelter and Berman, 2009).

In this report, we investigated the control of cell division during plant infection by the rice blast fungus *Magnaporthe oryzae*. Rice blast destroys up to 18% of the annual rice (*Oryza sativa*) harvest and represents a considerable threat to global food security (Wilson and Talbot, 2009). The disease is initiated when *M. oryzae* forms specialized dome-shaped infection cells called appressoria, which are distinct, in both shape and cellular organization, from the cylindrical hyphae by which fungi normally grow (Dean, 1997; Wilson and Talbot, 2009). Appressoria develop enormous turgor of up to 8.0 MPa, and this pressure is translated into physical force to rupture the rice leaf cuticle, allowing invasion of plant tissue (Dean, 1997). Previously, we showed that mitosis is a prerequisite for appressorium development in *M. oryzae* (Veneault-Fourrey et al., 2006). A single round of nuclear division occurs shortly after spore germination on the rice leaf surface. One of the daughter nuclei migrates to the germ tube tip where the appressorium is formed, while the other nucleus migrates back into the conidial cell from, which its mother nucleus originated (Veneault-Fourrey et al., 2006). Following mitosis and nuclear migration, an appressorium is formed and the conidium undergoes autophagic, programmed cell death, during which its nuclei are degraded (Veneault-Fourrey et al., 2006; Kershaw and Talbot, 2009). A DNA replication-associated checkpoint is necessary for initiation of appressorium formation, whereas entry into mitosis is essential for differentiation of functional appressoria (Saunders et al., 2010). The checkpoints that regulate appressorium differentiation are therefore responsible for a precisely choreographed developmental program leading to plant infection, in which the single nucleus in the appressorium is the source for all subsequent genetic material in the fungus as it invades host plant tissue (Veneault-Fourrey et al., 2006; Saunders et al., 2010).

[1] Current address: The Sainsbury Laboratory, Norwich Research Park, Colney Lane, Norwich NR47UH, UK.
[2] Address correspondence to n.j.talbot@exeter.ac.uk.
The author responsible for distribution of materials integral to the findings presented in this article in accordance with the policy described in the Instructions for Authors (www.plantcell.org) is: Nicholas J. Talbot (n.j.talbot@exeter.ac.uk).
[W] Online version contains Web-only data.
www.plantcell.org/cgi/doi/10.1105/tpc.110.074492

In this study, we set out to investigate the position, orientation, and timing of infection-associated cell division in *M. oryzae*. We report here that appressorium development in *M. oryzae* involves spatial uncoupling of mitosis and cytokinesis. The cell division that leads to appressorium differentiation is defined initially by formation of a heteromeric septin ring complex before the onset of mitosis. Nuclear division is then followed by long-distance nuclear migration, which triggers development of an actomyosin contractile ring at the base of the nascent appressorium. We also demonstrate that conditional mutation of Sep1, a key spatial regulator of cytokinesis and nuclear division, is sufficient to prevent rice blast disease.

RESULTS

Live Cell Imaging of Mitosis during Appressorium Morphogenesis in *M. oryzae*

To investigate spatial regulation of cell division in *M. oryzae*, we first visualized the relative positions of nuclear division and subsequent cytokinesis by determining the position of the actomyosin contractile ring involved in septum formation (Bi et al., 1998; Bi, 2001; Harris, 2001). We introduced a tropomyosin:*eGFP* (for enhanced green fluorescent protein) gene fusion (Pearson et al., 2004) into a wild-type strain of *M. oryzae*, Guy-11 (Leung et al., 1988), expressing a histone H1:red fluorescent protein (RFP) gene fusion (Saunders et al., 2010) and performed live cell imaging of mitosis and cytokinesis. In hyphae of *M. oryzae*, we found that actomyosin ring formation was consistently associated with the position of the premitotic nucleus and the medial position of the spindle during nuclear division, as shown in Figure 1A. This occurred during both hyphal branching and subapical nuclear division within growing hyphae. To determine the spatial pattern of mitosis during appressorium formation, we incubated a conidial suspension of the *M. oryzae* H1:RFP strain on a hydrophobic glass surface and observed mitosis 4 to 6 h later (Figure 1B). Nuclear division always occurred in the germ tube, close to the site of germ tube emergence, 4 to 6 h after germination (Figure 1B; see Supplemental Movie 1 online). Staining with the lipophilic dye 3,3′-dihexyloxacarbocyanine iodide ($DiOC_6$) highlighted the nuclear envelope (Koning et al., 1993) as well as extensive endoplasmic reticulum throughout the germ tube. The nuclear envelope appeared to remain intact throughout nuclear division, consistent with a closed, or partially closed, mitosis occurring in *M. oryzae* as in other filamentous ascomycetes (Gladfelter and Berman, 2009; Ukil et al., 2009). However, migration of a daughter nucleus into the incipient appressorium was immediately followed by intense localization of tpmA:eGFP at the neck of the appressorium, perpendicular to the longitudinal axis of the germ tube (Figure 1C; see Supplemental Movie 2 online). Actomyosin ring formation at the site of cytokinesis was typically completed within 6 min of the preceding mitosis, whereas ring formation during septation in vegetative hyphae was observed to take 30 min (Figure 1). Actin then accumulated within the appressorium during its maturation, prior to formation of the penetration hypha that the fungus uses to rupture the plant cuticle, as shown in Supplemental Figure 1 online.

To test whether spatial uncoupling of nuclear division and cytokinesis is specific to appressorium development, we introduced *H1:eRFP* and *tpmA:eGFP* gene fusions into mutants defective in appressorium morphogenesis. The *M. oryzae* Δ*pmk1* mutant is unable to differentiate appressoria due to absence of the pathogenicity-associated mitogen-actived protein kinase and instead produces undifferentiated germ tubes (Xu and Hamer, 1996). Strikingly, we found that Δ*pmk1* mutants underwent numerous rounds of nuclear division within the germ tube in which actomyosin ring formation always occurred at the medial position between daughter nuclei, rather than at the hyphal apex, as shown in Figure 1D and Supplemental Figure 2 online. Similarly in Δ*cpkA* mutants, which form aberrant nonfunctional appressoria (Mitchell and Dean, 1995; Xu et al., 1997), cytokinesis also occurred predominantly at the midpoint between daughter nuclei (Figure 1D; see Supplemental Figure 1 online). *CPKA* encodes the cAMP-dependent protein kinase A catalytic subunit and is essential for appressorium function (Mitchell and Dean, 1995; Xu et al., 1997). By contrast, developmental mutants that form morphologically normal appressoria, such as Δ*mst12*, a transcription factor mutant unable to form penetration hyphae (Park et al., 2002), showed clear separation of mitosis and cell division with actomyosin ring formation at the neck of the incipient appressorium (Figure 1D; see Supplemental Figure 2 online). We conclude that spatial uncoupling of mitosis and cytokinesis is specifically associated with the morphogenetic program for appressorium differentiation in *M. oryzae*.

Septin Ring Formation Precedes Mitosis during Appressorium Morphogenesis by *M. oryzae*

To investigate the relationship between mitosis and septation during appressorium development, we decided to determine the positions and times at which septin complexes form during conidial germination and appressorium formation. Septins are conserved cytoskeletal GTPases that were first described in the budding yeast *Saccharomyces cerevisiae* and fulfill diverse functions, forming heteromeric complexes that assemble as filaments, gauzes, or ring structures. They interact with membranes, actin, and microtubules and serve as organizational markers during cell division and polarized growth, in addition to being components of the morphogenesis and spindle position checkpoints (Lew, 2003; Douglas et al., 2005; Gladfelter and Berman, 2009). At a prospective bud site, the core septins Cdc3, Cdc10, Cdc11, and Cdc12 form a ring, which then develops into an hourglass-shaped collar at the mother-bud neck, before splitting into two rings during cytokinesis (Gladfelter et al., 2005, 2006). In filamentous fungi, septins assemble into a wider variety of complexes that form at growing hyphal tips, hyphal branch points, the bases of cellular protrusions, and, importantly, at sites of future septum formation. In *Aspergillus nidulans*, four of the five septins, AspA, AspB, AspC, and AspD, form a heteropolymeric complex, which appears as a ring or collar at the base of an emerging germ tube shortly after conidial germination. This septin ring is formed postmitotically and provides the first positional cue for the subsequent site of septation (Westfall and Momany, 2002; Lindsey et al., 2010). We

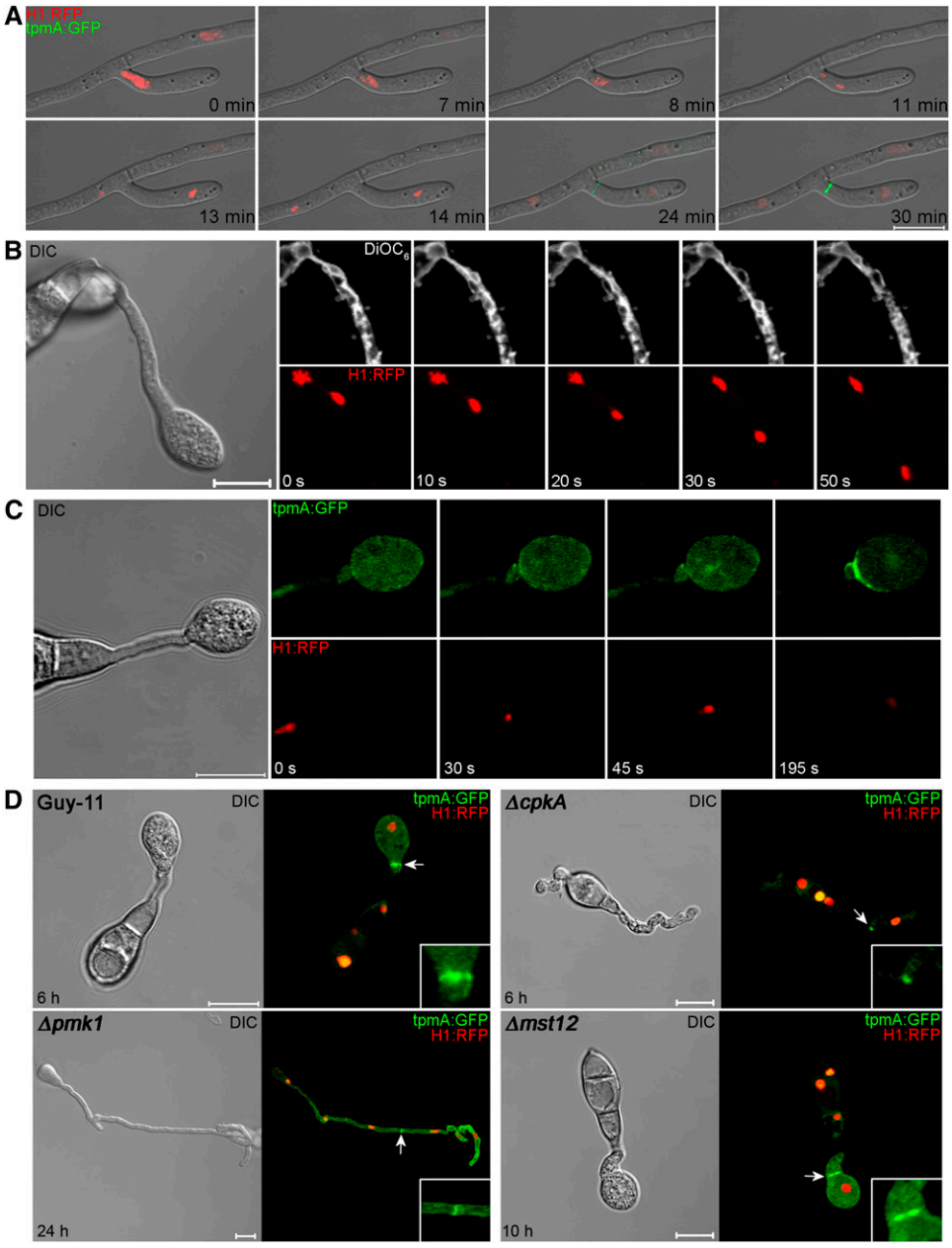

Figure 1. Spatial Uncoupling of Mitosis and Cytokinesis during Infection-Related Development in the Rice Blast Fungus *M. oryzae*.

(A) Laser confocal micrographs of a time series to show actomyosin ring formation in *M. oryzae* expressing tpmA:GFP and histone H1:RFP during vegetative hyphal growth. The site of septation in a hyphal branch occurs at the medial position of the preceding nuclear division.

(B) Time series of micrographs showing mitosis occurring during appressorium development by *M. oryzae*. Conidial suspensions of the *M. oryzae* H1:RFP strain were prepared and the lipophilic stain $DiOC_6$ used to stain the nuclear envelope. A differential interference contrast (DIC) image of the whole germ tube and developing appressorium is shown in the left panel.

(C) Time series to show actomyosin contractile ring formation during differentiation of the appressorium in *M. oryzae* tpmA:GFP-Histone H1:RFP strain. Left panel shows DIC image of the nascent appressorium. Right panels show TpmA:GFP and H1:RFP signals, respectively.

(D) Micrographs of *M. oryzae* strain Guy-11, Δ*cpkA*, Δ*pmk1*, and Δ*mst12* mutants expressing H1:RFP, and tpmA:GFP gene fusions incubated on cover slips to allow appressorium development. Septation was spatially separated from the site of nuclear division only in Guy-11 and the Δ*mst12* strains, which are competent in appressorium formation. All images were recorded using a Zeiss LSM510 Meta laser confocal laser scanning microscope system.

Bars = 10 μm.

therefore identified a family of six putative septin-encoding genes from the *M. oryzae* genome. We characterized two of these genes; *SEP4*, which shows 55% identity and 76% similarity to Cdc10 from *S.cerevisiae*, and *SEP5*, which is 44% identical and 64% similar to Cdc 11 (see Supplemental Figure 3 online). *SEP4* and *SEP5* gene fusions with GFP were constructed and expressed under their native promoters in a *M. oryzae* strain expressing H1:RFP (Saunders et al., 2010) to investigate the relationship between nuclear division and septin ring formation. We observed that a septin ring was formed at the base of the germ tube, proximal to the conidium, within 2 h of germination and a second septin ring developed at the neck of the developing appressorium, 4 h after germination, as shown in Figure 2. Interestingly, septin ring formation at the future site of septum formation always occurred before the onset of mitosis (Figure 2B). Septin rings dispersed, or were degraded, soon afterwards, and only very small numbers of germlings had clear septin rings after 8 h, during appressorium maturation. We conclude that the appressorium septation site is defined at an early stage following spore germination by formation of a heteromeric septin ring complex, which precedes mitosis in the germ tube.

Genetic Analysis of the Role of Cytokinesis and Septation during Infection-Related Morphogenesis

To test the biological relevance of the observed pattern of cytokinesis, we investigated the genetic control of septation. In the fission yeast *Schizosaccharomyces pombe*, the septation initiation network consists of a suite of proteins that monitors mitotic progression and coordinately initiates cytokinesis (Bardin and Amon, 2001). The *S. pombe* Cdc7 septation initiation network protein is a Ser-Thr kinase necessary for septum formation (Fankhauser and Simanis, 1994). Cdc7 shows 42% identity to *A. nidulans* SepH (Bruno et al., 2001), which is required for septum development in the filamentous fungus, suggesting that this is a conserved regulatory function (Bruno et al., 2001; Harris, 2001). We reasoned that perturbation of Cdc7 function in *M. oryzae* would provide a test of the functional significance of infection-associated cytokinesis. We identified a putative Cdc7 homolog, Sep1, with 52% amino acid identity to *A. nidulans* SepH, as shown in Supplemental Figure 4 online. Sep1 has a protein kinase domain at its N terminus (residues 59 to 313) and a highly conserved region with 73% identity to the *A. nidulans* SepH kinase domain. We introduced *M. oryzae SEP1* into a temperature-sensitive *A. nidulans sepH1* mutant, and this restored its

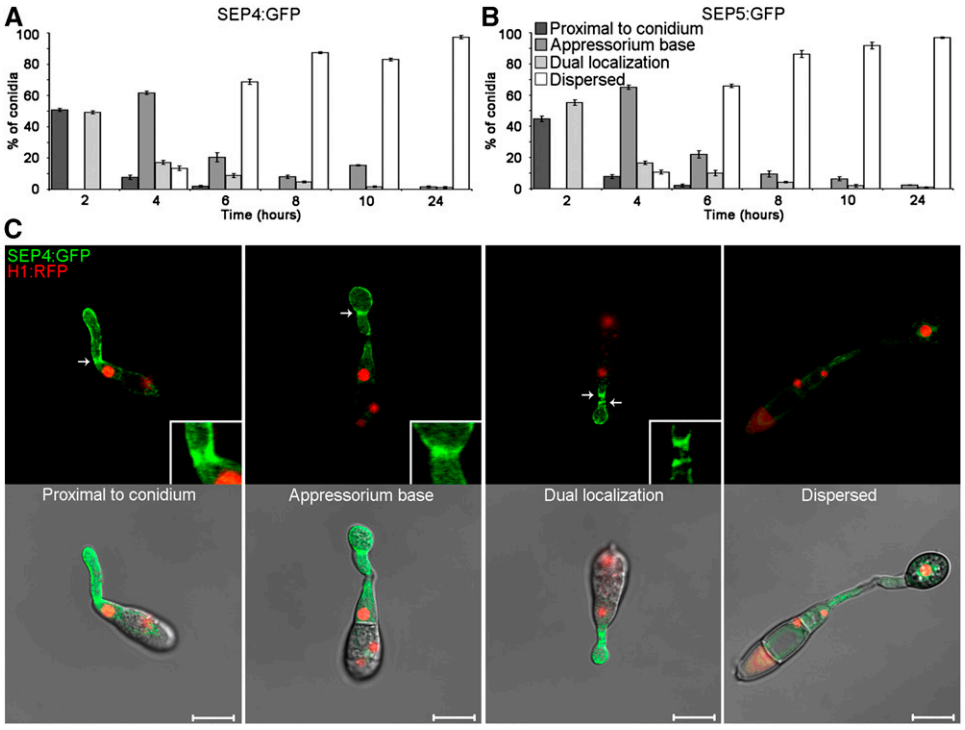

Figure 2. Septin Ring Formation Occurs Prior to Mitosis during Appressorium Development by *M. oryzae.*

Nuclear division and septin ring formation were visualized in *M. oryzae* by constructing *SEP4:GFP* and *SEP5:GFP* gene fusions and expressing these in a *H1:RFP*-expressing strain of Guy-11.

(A) and **(B)** Bar charts to show the frequency of septin complex formation by SEP4:GFP **(A)** or SEP5:GFP **(B)** during a time course of appressorium development. Values represent the mean, and the error bars represent 1 SE.

(C) Laser confocal microscopy to show septin ring formation at the base of the germ tube proximal to the conidium, at the base of incipient appressoria, dual localization to both of these positions, and the dispersal of septin complexes during appressorium maturation. Arrows indicate the positions of septin ring structures. All images were recorded using a Zeiss LSM510. Bars for all panels = 10 μm.

ability to form septa when vegetative hyphae were incubated at the nonpermissive temperature, as shown in Figure 3A, indicating that the proteins are functionally related.

To test the role of Sep1 in *M. oryzae*, we generated a temperature-sensitive allele of the gene analogous to the *A. nidulans sepH1* temperature-sensitive mutation, which has a Gly-to-Arg substitution at codon 793 (Bruno et al., 2001). The mutation was generated in *M. oryzae SEP1* (Figure 3B) and the resulting allele introduced into the fungus by targeted allelic replacement. We generated 24 *sep1*^{G849R} transformants that displayed a hyphal growth defect at 32°C, but which could be partially restored by subsequent incubation at 24°C (Figure 3C). DNA gel blot analysis and genomic DNA sequencing allowed selection of two transformants (76 and 169) containing single homologous insertions of the *sep1*^{G849R} allele. One of these transformants, 76, was subjected to a second transformation to introduce the *H1:eRFP* gene fusion, enabling us to assess the effect of the *sep1*^{G849R} mutation on nuclear division.

We quantified septum formation and nuclear number in *sep1*^{G849R} mutants compared with the isogenic H1:RFP strain of *M. oryzae*. Conidial suspensions were incubated in a moist chamber at 24°C or, after 1 h, transferred to a semirestrictive temperature of 29°C, which does not interfere with appressorium formation (Veneault-Fourrey et al., 2006). Surprisingly, calcofluor white staining revealed an increased frequency of septation in the germ tube during appressorium development of the *M.*

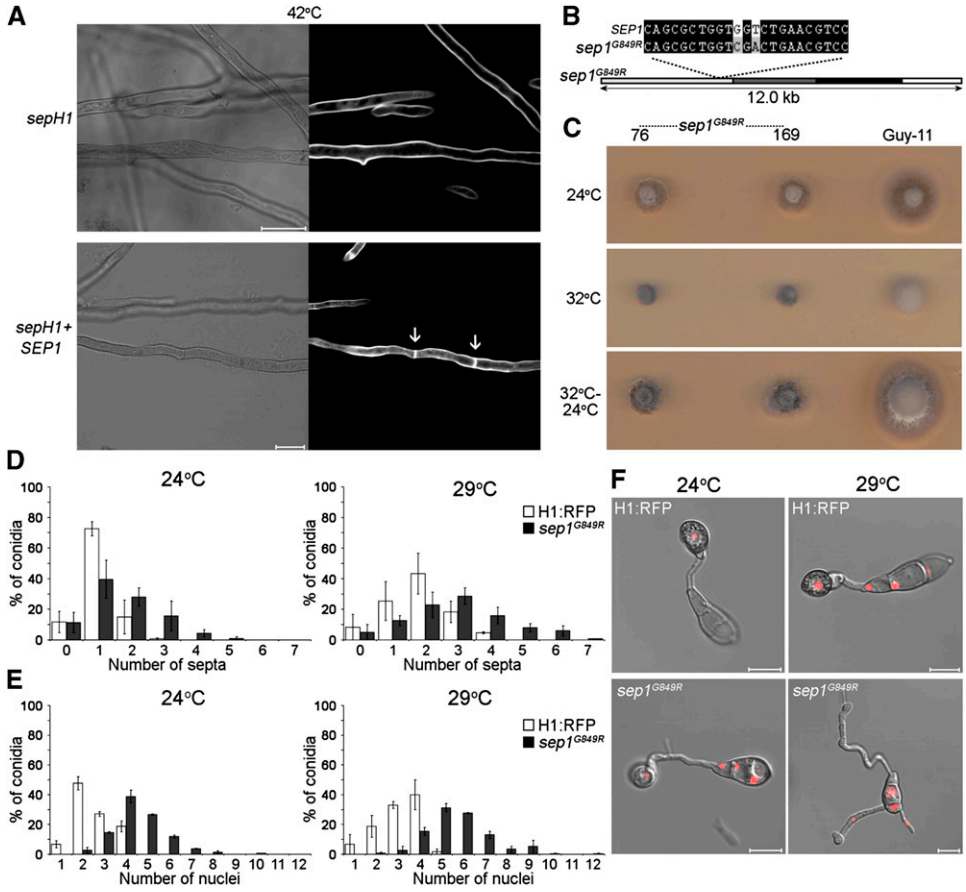

Figure 3. *SEP1* Is a Spatial Regulator of Cytokinesis in *M. oryzae.*

(A) *M. oryzae SEP1* is a functional homolog of the *A. nidulans sepH* septation gene. The *M. oryzae SEP1* gene was expressed in an *A. nidulans sepH1* thermosensitive mutant under the native SepH promoter and restored its ability to form septa at 42°C, as shown by calcofluor white staining (right panels; light micrographs are on the left).

(B) Schematic representation of the *sep1*^{G849R} allele, which was introduced into *M. oryzae* Guy-11 by homologous recombination.

(C) Thermosensitivity of the *sep1*^{G849R} mutant of *M. oryzae*. Plugs of mycelium (5-mm diameter) from putative *sep1*^{G849R} transformants, and Guy-11, were incubated at 24 or 32°C for 4 d. Restoration of hyphal growth was assessed by incubation for a further 3 d at 24°C.

(D) Quantitative analysis of infection-associated septation in *sep1*^{G849R} mutants. The *grg(p):H1:eRFP* vector was introduced into the *M. oryzae sep1*^{G849R} strain. Conidial suspensions were then prepared from the *M. oryzae* H1:RFP and *sep1*^{G849R} strains and allowed to form appressoria at 24 or 29°C. After 10 h, the number of septa was recorded following calcofluor white staining.

(E) Quantitative analysis of nuclear number in *sep1*^{G849R}. Conidial suspensions were allowed to form appressoria at 24 or 29°C, and nuclear number was recorded after 10 h.

(F) Representative images of nuclear distribution during appressorium morphogenesis of *sep1*^{G849R}. Bars = 10 μm; error bars are 1 SE.

oryzae sep1^{G849R} mutant, as shown in Figure 3D (see Supplemental Figure 5 online). This suggests that, in contrast with *A. nidulans* SepH (Bruno et al., 2001), Sep1 may act as a negative regulator of cytokinesis in *M. oryzae*. However, we also observed multiple septa in two wild-type strains that expressed a copy of the *sep1^{G849R}* allele (as well as a functional copy of *SEP1*) when these were incubated at 29°C (see Supplemental Figure 6 online). This suggests that the *sep1^{G849R}* allele might have a dominant effect on the regulation of septation. Consistent with this idea, the *SEP1 sep1^{G849R}* strains showed reduced growth in culture compared with the isogenic wild-type Guy-11 (see Supplemental Figure 7 online) but did not show the severe temperature-sensitive phenotype of *sep1^{G849R}* mutants (Figure 3). Interestingly, we observed that the cell cycle arrest of nuclei in nongerminating cells of the three-celled conidium of the *sep1^{G849R}* mutant was alleviated because nuclear number increased rapidly, as shown in Figures 3E and 3F and Supplemental Figure 8 online. In spite of the misregulation of germ tube morphology and nuclear division in *sep1^{G849R}* mutants, the frequency of appressorium development was indistinguishable from that of the wild-type Guy-11 (Figure 4A), although germ tubes were elongated and branched (Figure 4B).

To test the ability of *sep1^{G849R}* appressoria to cause rice blast disease, we inoculated the blast-susceptible rice cultivar CO-39. The density of disease lesions on rice leaves inoculated with the *sep1^{G849R}* strain was significantly reduced at the semirestrictive temperature of 29°C, as shown in Figure 4C (two-sample *t* test assuming equal variances, $t = 9.35$, $df = 10$, $P < 0.05$), although no reduction was observed at the permissive temperature of 24°C compared with Guy-11 (Figure 4C; two-sample *t* test assuming equal variances, $t = 1.41$, $df = 16$, $P > 0.05$). When considered together, these results suggest that spatial control of septation is necessary for development of infection-competent appressoria by the rice blast fungus.

SEP1 Is a Dose-Dependent Regulator of Nuclear Division

A conditional mutation in *SEP1* increased septation and nuclear division during appressorium morphogenesis. We therefore hypothesized that overexpression of *SEP1* might, conversely, prevent cytokinesis and enable us to investigate the requirement for cytokinesis during appressorium development. To test this, we placed *SEP1* under control of the isocitrate lyase gene promoter [$ICL1_{(p)}$] to enable induction of gene expression by acetate (Wang et al., 2003) and introduced the *ICL1(p):SEP1* gene fusion into the *M. oryzae* H1:RFP strain. Two putative *ICL1 (p):SEP1* transformants were identified carrying either single or multiple insertions of the fusion construct. The two transformants, SEP1-1 and SEP1-9, grew normally in culture in the presence or absence of acetate, as shown in Figure 5A. During conidial germination and appressorium development, inducible overexpression of *SEP1* increased nuclear number rapidly as a consequence of alleviating the cell cycle arrest of nuclei within nongerminating conidial cells (Figures 5B and 5C; see Supplemental Figure 9 online). When considered with analysis of the *sep1^{G849R}* mutant, these results are consistent with requirement for a steady state level of Sep1 protein to maintain the inherent cell cycle arrest phenotype in nongerminated conidial cells during infection-related development. Inducible overexpression of *SEP1* did not, however, affect septation (Figure 5D; see Supplemental Figure 10 online). We conclude that normal Sep1 function, which is adversely affected by the *sep1^{G849R}* allele even in a heterozygous state, is necessary to coordinate the spatial control of septation in *M. oryzae*, regardless of its abundance. The frequency of appressorium development in SEP1-1 and SEP1-9 was, however, identical to that of the wild type as shown in Figure 5E, with no associated germ tube–specific morphological defect (Figure 5F). Correct *SEP1* function is therefore necessary for spatial control of septation but also for maintaining the

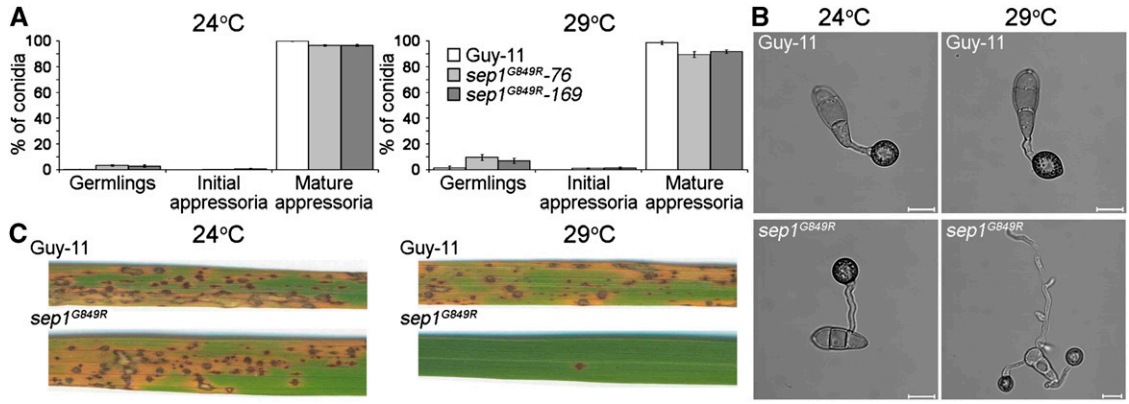

Figure 4. *SEP1* Is Required for Appressorium-Mediated Plant Infection by *M. oryzae*.

(A) Bar charts to show the frequency of appressorium development in *M. oryzae sep1^{G849R}* temperature-sensitive mutants. Error bars are 1 SE.

(B) Conidial suspensions of two independent *M. oryzae sep1^{G849R}* transformants were incubated in conditions to allow appressorium development, which was recorded after 24 h. Bars = 10 μm.

(C) *M. oryzae sep1^{G849R}* mutants were unable to cause rice blast disease. Leaves from the dwarf Indica rice (*O. sativa*) cultivar, CO-39, following inoculation with 5×10^4 spores mL^{-1} of a *sep1^{G849R}* mutant and Guy-11. Following inoculation, rice plants were incubated initially for 24 h at either the permissive temperature of 24°C or a semirestrictive temperature of 29°C. All plants were then transferred to 24°C and leaves harvested 5 d later.

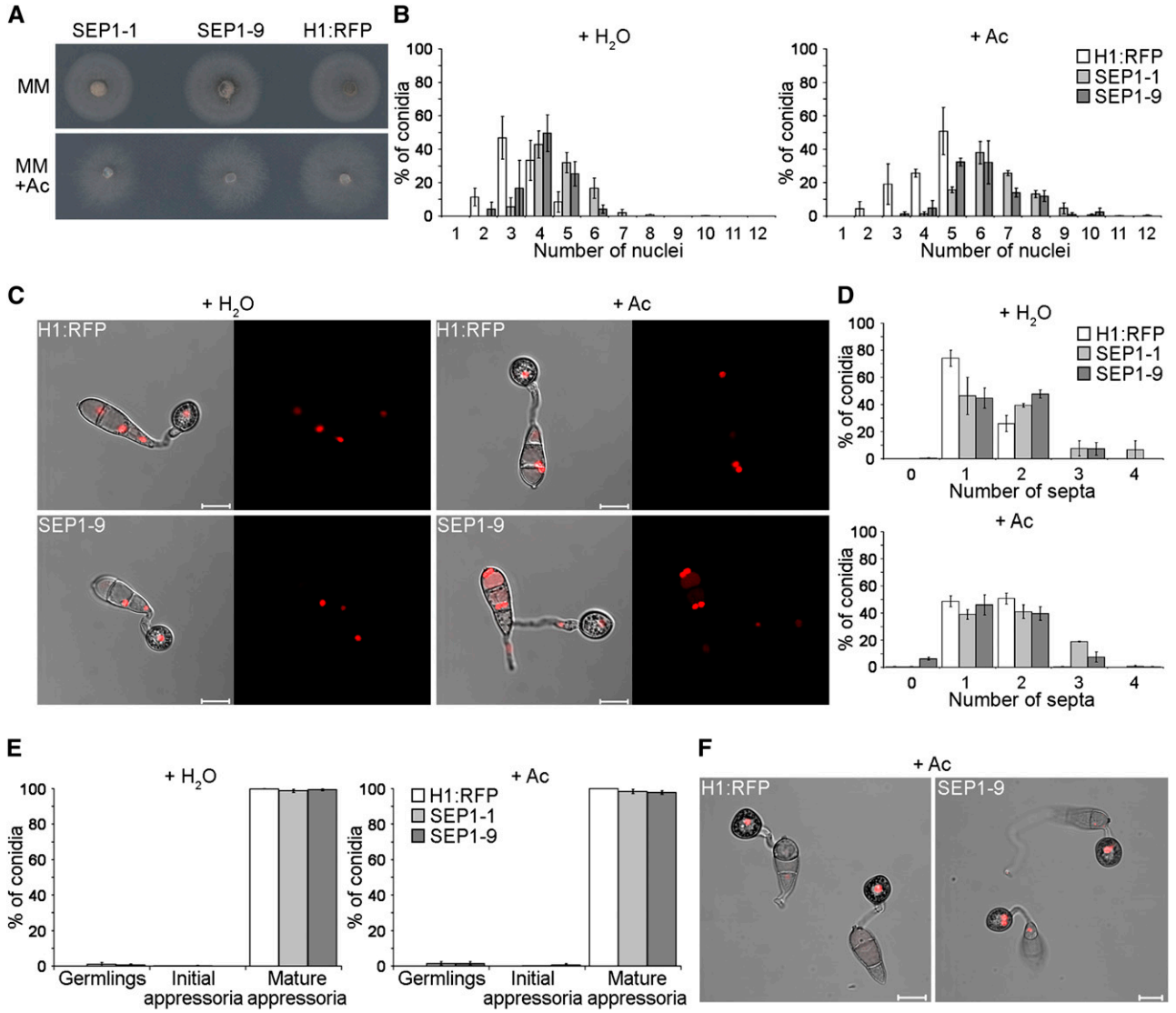

Figure 5. Inducible Overexpression of *SEP1* in *M. oryzae* Leads to Aberrant Nuclear Division.

SEP1 was placed under control of the isocitrate lyase gene promoter sequence to enable induction of gene expression by acetate. Two transformants were isolated, one containing multiple insertions of the *ICL1(p):SEP1* construct, SEP1-1, and one containing a single insertion of the transgene, SEP1-9. Ac, sodium acetate; bars =10 μm; error bars are 1 SE.

(A) Vegetative growth of SEP1-1 and SEP1-9 transformants. Plugs of mycelium (5-mm diameter) from the SEP1-1 and SEP1-9 strains and the isogenic H1:RFP strain were used to inoculate minimal medium (MM) with or without 50 mM sodium acetate. Hyphal growth was assessed 4 d later.

(B) Quantitative analysis of nuclear number in H1:RFP, SEP1-1, and SEP1-9. Conidial suspensions were prepared and incubated to allow appressorium development in the presence or absence of acetate. Nuclear number was recorded 10 h later.

(C) Representative images to show nuclear distribution during appressorium morphogenesis.

(D) Quantitative analysis of septum formation during appressorium morphogenesis. Conidial suspensions were stained with calcofluor white after 10 h and the number of septa recorded.

(E) Bar charts to show the frequency of appressorium development in the presence or absence of acetate. Appressorium development was recorded 24 h after inoculation.

(F) Representative images of appressorium formation.

cell cycle arrested state of nuclei in nongerminating cells of *M. oryzae* spores. The septation-associated role of *SEP1* is necessary for appressorium-mediated plant infection by the rice blast fungus.

DISCUSSION

In this study, we aimed to determine the relationship between nuclear division and cytokinesis during formation of appressoria by a plant pathogenic fungus. Previous analysis has shown that development of appressoria in the rice blast fungus requires a morphogenetic program regulated by the cAMP response pathway and the Pmk1 MAP kinase cascade in response to the hard, hydrophobic rice leaf surface and absence of exogenous nutrients (Dean, 1997; Wilson and Talbot, 2009). In response to these signals, a germinating conidium undergoes a single round of mitosis, which is a necessary prerequisite for appressorium differentiation as evidenced by the fact that a conditional *nimA* mutant, blocked at mitotic entry, fails to differentiate functional infection cells (Veneault-Fourrey et al., 2006; Saunders et al., 2010).

Our first conclusion from this study is that in *M. oryzae*, spatial uncoupling of nuclear division and septation occurs during appressorium development, distinguishing it from cytokinesis during hyphal growth of the fungus. In hyphae of *M. oryzae*, the position of cell division coincides with the medial position of the preceding mitosis, defining the position of the subsequent septum and leading to an even distribution of cellular compartments along the hypha with relatively uniform intercalary length and an even distribution of nuclei. During appressorium differentiation, nuclear division and cytokinesis are, instead, spatially separated, and transit of the nucleus to the swollen hyphal tip always precedes differentiation and cytokinesis of the appressorium (see Supplemental Movie 2 online). By contrast, germ tubes of Δ*pmk1* and Δ*cpkA* mutants, which do not differentiate functional appressoria (Mitchell and Dean, 1995; Xu and Hamer, 1996), undergo coupled mitosis and cytokinesis, which is identical to the pattern observed in hyphae. Considering these results together suggests that the spatial relationship between mitosis and cytokinesis is a component of the morphogenetic program leading to appressorium formation.

The site of cell division in fungi is normally determined early in the cell cycle (Gladfelter and Berman, 2009; Oliferenko et al., 2009). In *S. cerevisiae*, for instance, cells divide by budding, and the site of bud assembly is determined in G1 by landmark proteins, such as Bud3p, Bud4p, Bud10p, and Axl1p (Casamayor and Snyder, 2002). These proteins recruit the GTPase Bud1p, which in turn recruits the guanine nucleotide exchange factor protein Cdc24p that acts on Cdc42p-GTPase, ultimately leading to assembly of septins (Cdc3, Cdc10, Cdc11, Cdc12, and Shs1) at the future site of cytokinesis (Park et al., 1997; Barral et al., 2000; Schuyler and Pellman, 2001). Budding yeast then has a mechanism to ensure that the mitotic spindle is correctly oriented across the mother-bud neck so one daughter nucleus successfully migrates into the bud before cell division. This process involves microtubule-associated proteins, Kar9 and Bim1, and a dynein Dyn1p, which has a key role in nuclear positioning, providing the main force that pulls the nucleus via astral microtubules (Schuyler and Pellman, 2001; Yeh et al., 2000; see model in Figure 6). If the spindle is not correctly oriented across the mother-daughter cell junction, this delays activation of the mitotic exit network, which prevents cytokinesis from occurring (Yeh et al., 2000; Schuyler and Pellman, 2001; Lew, 2003). Cytokinesis is therefore dependent on the correct positioning of nuclear division. In the fission yeast *S. pombe*, the cell division site is determined late in G2 by position of the premitotic nucleus, leading to fission of the cell across its equatorial plane and generation of two equally sized daughter cells (Bähler and Pringle, 1998; Bähler et al., 1998). In the filamentous fungus *A. nidulans* during spore germination, asymmetric division delimits the extending germ tube from the spore, coincident with completion of the third nuclear division (Kaminskyj, 2000; Harris, 2001). The septum in *A. nidulans*, however, assembles at a point equidistant from each daughter nucleus in response to signals that appear to originate from the mitotic spindle during nuclear division (Wolkow et al., 1996). Spatial separation of nuclear division and cytokinesis in *M. oryzae* is therefore very unusual indeed (Figure 6), with very few previous examples reported (Straube et al., 2005; Gladfelter et al., 2006).

It was particularly significant that deposition of the septin ring, which provides the first organization cue for cytokinesis, defines the position of the appressorium septum, prior to mitosis in the germ tube. This is consistent with the spatially separate position of cell division being identified at a very early stage in the cell cycle (Gladfelter and Berman, 2009). Recently, we demonstrated that the initiation of appressorium formation in *M. oryzae* requires premitotic DNA replication to have occurred because treatment of germlings with hydroxyurea, which inhibits DNA replication and causes G1 arrest, prevents differentiation of germ tube tips (Saunders et al., 2010). Moreover, a *nim1* temperature-sensitive mutant that prematurely enters mitosis in the absence of DNA replication is unable to initiate appressorium development (Saunders et al., 2010). The temporal pattern of septin ring formation that we observed in this study is therefore consistent with septin regulation by the DNA replication checkpoint that initiates appressorium morphogenesis in *M. oryzae*. The premitotic control of septin ring formation following conidial germination contrasts with previous observations in *A. nidulans* where the AspB septin has been shown, for instance, to contribute to ring formation under postmitotic control (Westfall and Momany, 2002), although premitotic control of septin complex formation does occur during hyphal branching (Westfall and Momany, 2002; Lindsey et al., 2010). Further investigation of the septin gene family in *M. oryzae* may prove to be very valuable in view of their diverse roles in cell division control, polarized growth, cell surface organization, exocytosis, and vesicle fusion, all of which are likely to be necessary virulence-associated functions in the fungus. Consistent with this idea, septins have found to be important for virulence of a number of fungal species (Boyce et al., 2005; Douglas et al., 2005; Gonzalez-Novo et al., 2006; Kozubowski and Heitman, 2010).

To test whether control of appressorium septation might be significant in the developmental program for plant infection, we perturbed the spatial regulation of cytokinesis and showed that this prevents *M. oryzae* from carrying out plant infection. The *M. oryzae sep1*^{G849R} mutant was predicted to impair cytokinesis

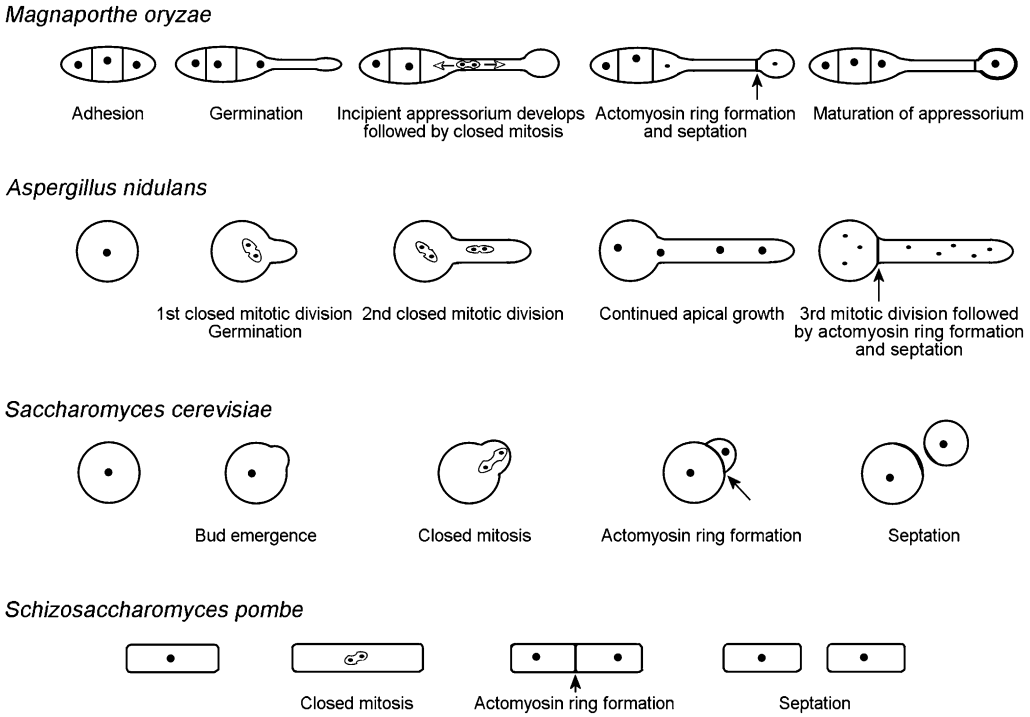

Figure 6. Spatial Uncoupling of Mitosis and Cytokinesis Is Associated with Appressorium Formation in the Rice Blast Fungus *M. oryzae*.

Schematic diagram to show the position and organization of septum formation in *M. oryzae* during appressorium development. The site of septation is spatially separated from the previous nuclear division. This contrasts with common patterns of septation in fungi, in which nuclear division is associated with the subsequent site of cytokinesis and septation. This occurs during spore germination in *A. nidulans*, budding of *S. cerevisiae*, and fission of *S. pombe*. Closed arrows indicate position of actomyosin ring formation; open arrows indicate direction of nuclear movement; nuclei are represented by closed circles.

based on previous analysis in *A. nidulans* (Bruno et al., 2001), but the equivalent *M. oryzae* mutant displayed enhanced septation at the restrictive temperature, perhaps due to a dominant-negative effect of the temperature-sensitive allele. Cell cycle arrest of nongerminating conidial cells was also alleviated, resulting in multiple nuclei being present in spores of the *sep1*^{G849R} mutant. Interestingly, in spite of undergoing nuclear division, these conidial cells did not germinate, showing that dormancy was not affected. The *A. nidulans* mutant *sepH1* has no such effect on nuclear division at its restrictive temperature (Bruno et al., 2001), suggesting a divergence in function in *M. oryzae*. Significantly, we observed that appressoria of the *sep1*^{G849R} mutant could not cause plant disease at a semi-restrictive temperature. Therefore, it is apparent that coordination of either nuclear or cellular division, or indeed both, is essential in preserving the functional competency of *M. oryzae* appressoria. Recently, we showed that the pivotal checkpoints that regulate appressorium morphogenesis occur prior to mitosis at S-phase and at mitotic entry (Saunders et al., 2010). By contrast, we found that arresting mitotic exit does not affect the frequency of appressorium formation but does affect the ability of infection cells to repolarize and cause plant infection. In this study, we have shown that septation initiation, which is linked to mitotic exit, is also not a prerequisite for appressorium morphogenesis but is essential for penetration peg formation and subsequent plant infection. The formation of a septum to separate the differentiated appressorium from the germ tube is likely to be essential for generation of the enormous turgor that is built up during cuticle penetration (de Jong et al., 1997; Thines et al., 2000). It is also possible that septation is a necessary prerequisite for cell wall differentiation and melanization that are necessary for appressorium function (Chumley and Valent, 1990; Tucker et al., 2004)

Our final conclusion is that Sep1 has a dual function in coordinating cytokinesis, which is independent of Sep1 abundance, and also nuclear division, but here in a Sep1 dose-dependent manner. Overexpression of Sep1, for instance, did not affect septation but instead led to release of the cell cycle arrest of nuclei in nongerminating conidial cells. Alleviation of such a cell cycle arrest phenotype has not previously been observed in *sepH*/*cdc7* mutants (Fankhauser and Simanis, 1994). In *S. pombe*, for example, deletion of *cdc7*, which is a component of the septation initiation network, produces highly elongated, multinucleate cells as a consequence of the inability to form septa, rather than resulting from a direct effect of Cdc7 on nuclear division (Fankhauser and Simanis, 1994). In addition, overexpression of Cdc7 initiated a multiple-septa phenotype (Fankhauser and Simanis, 1994). Similarly, in *S. cerevisiae*, deletion or overexpression of the Sep1 homolog CDC15, a component of the mitotic exit network, inhibited or disrupted

actin ring formation, blocking subsequent septum formation with a consequent cell cycle arrest phenotype (Cenamor et al., 1999). Therefore, dose-dependent cell cycle regulation by Sep1 in *M. oryzae* represents a previously unknown signaling mechanism for coordination of cell cycle progression during spore germination, infection structure formation, and plant infection.

METHODS

Fungal Strains, Growth Conditions, Pathogenicity, and Infection-Related Development Assays

Isolates of *Magnaporthe oryzae* (Couch and Kohn, 2002; formerly *M. grisea*) used in this study are stored in the laboratory of N.J.T. (University of Exeter, UK). Previously described strains are listed in Supplemental Table 1 online, and those generated in this study are in Supplemental Table 2 online. All strains were routinely maintained on complete medium (Talbot et al., 1993). DNA-mediated transformation, genomic DNA extractions, and plant infection assays were performed as described previously (Talbot et al., 1993). Conidial germination and development of appressoria were monitored on hydrophobic borosilicate glass cover slips (Hamer et al., 1988). A conidial suspension of 5×10^4 conidia mL^{-1} was placed onto the surface of glass cover slips and then incubated in a moist chamber at 24°C.

Microscopy Methods

All images acquired during hyphal growth, germination, and appressorium development were recorded using a Zeiss LSM510 Meta confocal laser scanning microscope system. Slides were prepared by sealing the cover slip with adhered conidia, with Vaseline petroleum jelly. Blue diode (405 nm), argon (458, 477, 488, and 504 nm), helium-neon (He-Ne; 543 nm), and He-Ne (633 nm) lasers were used to excite the various fluorochromes, and all images recorded following examination under the ×63 oil objective. Offline image analysis was performed using the LSM image browser (Zeiss) or MetaMorph 7.5 (Molecular Devices). The confocal laser scanning microscope multitrack setting was used to enable synchronized image acquisition.

The lipophilic stain $DiOC_6$ (AnaSpec) was used to stain the nuclear envelope (Koning et al., 1993). A conidial suspension of 5×10^4 conidia mL^{-1} from the *M. oryzae* H1:RFP strain was applied to cover slips in a moist chamber at 24°C. A 10 mM stock solution of $DiOC_6$ was prepared in DMSO and a 10μM $DiOC_6$ aliquot added to the conidial suspension.

tpmA:eGFP Fusion Plasmid Construction

The 2.8-kb modified *M. oryzae ILV1* allele, conferring resistance to sulfonylurea, was amplified with primers 5SU and 3SU from pCB1532 (Sweigard et al., 1997). Sequences of all primers are shown in Supplemental Table 3 online. The resulting 2.8-kb amplicon was introduced into the *tpmA:eGFP* gene fusion vector pCP32 (Pearson et al., 2004), kindly provided by Steven Harris (University of Nebraska, Lincoln, NE) and introduced into a *H1:eRFP*-expressing Guy-11 strain of *M. oryzae* (Saunders et al., 2010). The *tpmA:eGFP* vector was also introduced into Δ*cpkA*, Δ*mst12*, and Δ*pmk1* mutants of *M. oryzae*, all in the same isogenic strain background, Guy-11. All transformants were assessed by DNA gel blot analysis and observations confirmed with at least two independent transformants.

Generation of *Sep4:eGFP* and *Sep5:eGFP* Gene Fusions

The *SEP4* and *SEP5* genes were identified from the *M. oryzae* genome sequence database and amplified from genomic DNA of strain Guy-11 with primers SEP4-F/SEP4-R and SEP5-F/SEP5-R (see Supplemental Table 3 online) and transformed with *Hin*dIII-digested pYSGFP-1 into *Saccharomyces cerevisiae*. Gene fusions were constructed by yeast gap repair cloning, based on homologous recombination in yeast (Oldenburg et al., 1997). Resulting plasmids were introduced in *M. oryzae* strain Guy-11 expressing H1:eRFP and assessed by DNA gel blot analysis. All experimental observations were confirmed with at least two independent transformants.

SEP1 Genomic Cloning, Plasmid Construction, and Complementation

A 7.2-kb gene fragment spanning the *SEP1* locus was amplified from genomic DNA with primers 5SepH-ts1-KpnI and 3SepH-KpnI. The *SEP1* fragment was ligated into the *Kpn*I site of pCB1004 (Carroll et al., 1994) and the resulting vector, pDS100, used to transform the *Aspergillus nidulans sepH1* mutant (Bruno et al., 2001).

Five putative *A. nidulans sepH1* transformants were selected and assessed for insertion of a single copy of *SEP1* by DNA gel blot. Each transformant was then analyzed for restoration of septation at 42°C. Septa were visualized with 0.4 μg mL^{-1} calcofluor solution as previously described (Veneault-Fourrey et al., 2006).

The *Mosep1^{G849R}* Gene Replacement Vector

To generate the *Mosep1^{G849R}* gene replacement vector, a genomic clone spanning *SEP1* (pDS100) was amplified using primers 5SepH-ts1-KpnI and 3SepH-ts1-NotI. The *ILV1* selectable marker was amplified with primers 5SU-ts-NotI and 3SU-ts-NotI and inserted downstream of the 3′ untranslated region (UTR) of *SEP1*. A 2.6-kb fragment of *SEP1* was amplified from a unique *Nde*I site within *SEP1* to the end of the *SEP1* 0.5-kb 3′UTR fragment with primers 5SepH-ts2-NotI and 3SepH-ts2-XbaI. The resulting 2.6-kb amplicon was gel purified and ligated to pGEM-T (Promega). The 2.6-kb fragment was subject to site-directed mutagenesis (Invitrogen) with primers 5SepH-ts3-NdeI and 3SepH-ts1-NotI to introduce two single-base substitutions; nucleotide 3175 was changed from guanine to cytosine to bring about a Gly-to-Arg substitution and a second silent mutation at nucleotide 3177 substituted thymine with adenine to generate a unique *Sal*I site to enable rapid screening of the resulting mutation. The mutagenesis procedure was performed according to the manufacturer's protocol (Invitrogen). Positive clones were identified by digestion with *Sal*I and the G849R mutation confirmed by DNA sequence analysis.

A 2.0-kb region adjacent and downstream of *SEP1* was introduced into pCR 2.1-TOPO containing the 7.2 kb *sep1^{G849R}* gene replacement fragment. The 2.6-kb *sep1^{G849R}* region was excised from pGEM-T and ligated into pCR 2.1-TOPO containing the 7.2-kb *SEP1* gene replacement fragment and the 2.0-kb region adjacent and downstream of *SEP1* to create pDS101. The 2.8-kb modified *ILV1* cassette was introduced into pDS101 and the resulting vector, pDS102, digested with *Kpn*I and *Xba*I, gel purified, and introduced into Guy-11. Potential *sep1^{G849R}* transformants were selected by DNA gel blot and sequence analysis. Two transformants were selected and transformed with the *grg(p):H1:eRFP* gene fusion to allow visualization of nuclei.

Regulated Expression of the *M. oryzae SEP1* Gene

A 1.5-kb *ICL1* promoter fragment, *ICL1(p)*, which drives expression of the isocitrate lyase-encoding gene, was amplified with primers 5ICL1P-NotI and 3ICL1P-SepH from a *ICL1(p):sGFP* fusion construct (Wang et al., 2003). A 5.7-kb gene fragment including the 5.2-kb open reading frame of *M. oryzae SEP1* and 0.5 kb of 3′UTR was amplified from genomic DNA with primers 5SepH-ICL1P and 3SepH-NotI. The 1.5-kb *ICL1(p)* and 5.7-kb *SEP1* amplicons were joined by fusion PCR. The 7.2-kb *ICL1(p):SEP1* region was ligated to pCB1532 (Sweigard et al., 1997) and

subsequently used for fungal transformation of *M. oryzae* H1:eRFP (tdTomato). In *M. oryzae* strains expressing *SEP1* under the control of the *ICL1* promoter, hyphal growth and appressorium development were assessed in the presence or absence of 50 mM sodium acetate.

Accession Numbers

Sequence data from this article can be found in the GenBank/EMBL databases under the following accession numbers: *M. oryzae SEP1* (MGG04100), *M. oryzae SEP4* (MGG06726), *M. oryzae SEP5* (MGG03087), *M. oryzae ILV1* AF013601, *S. cerevisiae CDC10* (YCR002C), *S. cerevisiae CDC11* (YJR076C), and *A. nidulans SepH* (XM360771).

Supplemental Data

The following materials are available in the online version of this article.

Supplemental Figure 1. Live Cell Imaging of Nuclear Dynamics and Actomyosin Ring Formation in the *M. oryzae* Strains Guy-11 and Δ*cpkA*.

Supplemental Figure 2. Live Cell Imaging of Nuclear Dynamics and Actomyosin Ring Formation in the *M. oryzae* Strains Δ*pmk1* and Δ*mst12*.

Supplemental Figure 3. Alignment of the Predicted *M. oryzae* Sep4 and Sep5 Amino Acid Sequences with Cdc10 and Cdc11 from *S. cerevisiae*.

Supplemental Figure 4. Alignment of the Predicted *M. oryzae* Sep1 Amino Acid Sequence with *A. nidulans* SepH.

Supplemental Figure 5. A Temperature-Sensitive Mutation in *M. oryzae SEP1* Increases Septation Frequency during Appressorium Formation.

Supplemental Figure 6. The $sep1^{G849R}$ Allele Increases the Frequency of Septation during Appressorium Development Even in the Presence of a Wild-Type Copy of *SEP1*.

Supplemental Figure 7. The $sep1^{G849R}$ Allele Reduces Hyphal Growth but Has No Effect on Appressorium Development Even in the Presence of a Wild-Type Copy of *SEP1*.

Supplemental Figure 8. A Temperature-Sensitive Mutation in *M. oryzae SEP1* Alleviates the Cell Cycle Arrest Phenotype of Nongerminating Conidial Cells during Appressorium Development.

Supplemental Figure 9. Inducible Overexpression of *M. oryzae SEP1* Alleviates the Cell Cycle Arrest Phenotype of Nongerminating Conidial Cells during Appressorium Development.

Supplemental Figure 10. Inducible Overexpression of *M. oryzae SEP1* Has No Effect on Septation Frequency during Appressorium Development.

Supplemental Table 1. *M. oryzae* Strains Used in This Study.

Supplemental Table 2. *M. oryzae* Strains Generated in This Study.

Supplemental Table 3. Detailed Information of the Primers Used in This Study.

Supplemental Movie 1. Live Cell Imaging of Closed Mitosis during Appressorium Development in *M. oryzae*.

Supplemental Movie 2. Live Cell Imaging of Actomyosin Ring Formation during the Asymmetric Cellular Division Associated with Appressorium Development in *M. oryzae*.

ACKNOWLEDGMENTS

This work was supported by a grant to N.J.T. from the Biotechnology and Biological Sciences Research Council, a graduate fellowship to D.G.O.S. from the University of Exeter, and a Halpin Studentship in Rice Blast Research to Y.F.D. We acknowledge Steve Harris (University of Nebraska, Lincoln, NE) for providing tpmA:eGFP, *Aspergillus* mutants, and for valuable discussions, Gero Steinberg (University of Exeter, UK) for help with figures and movie preparation, and Richard Wilson (University of Nebraska, Lincoln, NE) for helpful discussions.

Received February 3, 2010; revised June 8, 2010; accepted June 28, 2010; published July 16, 2010.

REFERENCES

Bähler, J., and Pringle, J.R. (1998). Pom1p, a fission yeast protein kinase that provides positional information for both polarized growth and cytokinesis. Genes Dev. **12:** 1356–1370.

Bähler, J., Steever, A.B., Wheatley, S., Wang, Y.L., Pringle, J.R., Gould, K.G., and McCollum, D. (1998). Role of polo kinase and Mid1p in determining the site of cell division in fission yeast. J. Cell Biol. **143:** 1603–1616.

Bardin, A.J., and Amon, A. (2001). MEN and SIN: What's the difference? Nat. Rev. Mol. Cell Biol. **2:** 815–826.

Barral, Y., Mermall, V., Mooseker, M.S., and Snyder, M. (2000). Compartmentalization of the cell cortex by septins is required for maintenance of cell polarity in yeast. Mol. Cell **5:** 841–851.

Bi, E. (2001). Cytokinesis in budding yeast: the relationship between actomyosin ring formation and septum formation. Cell Struct. Funct. **26:** 529–537.

Bi, E., Maddox, P., Lew, D.J., Salmon, E.D., McMillan, J.N., Yeh, E., and Pringle, J.R. (1998). Involvement of an actomyosin contractile ring in *Saccharomyces cerevisiae* cytokinesis. J. Cell Biol. **142:** 1301–1312.

Boyce, K.J., Chang, H., D'Souza, C.A., and Kronstad, J.W. (2005). A *Ustilago maydis* septin is required for filamentous growth in culture and for full symptom development on maize. Eukaryot. Cell **4:** 2044–2056.

Bruno, K.S., Morrell, J.L., Hamer, J.E., and Staiger, C.J. (2001). SEPH, a Cdc7p orthologue from *Aspergillus nidulans*, functions upstream of actin ring formation during cytokinesis. Mol. Microbiol. **42:** 3–12.

Carroll, A.M., Sweigard, J.A., and Valent, B. (1994). Improved vectors for selecting resistance to hygromycin. Fungal Genet. Newsl. **41:** 22.

Casamayor, A., and Snyder, M. (2002). Bud-site selection and cell polarity in budding yeast. Curr. Opin. Microbiol. **5:** 179–186.

Cenamor, R., Jimenez, J., Cid, V.J., Mobela, C., and Sanchez, M. (1999). The budding yeast Cdc15 localizes to the spindle pole body in a cell-cycle-dependent manner. Mol. Cell Biol. Res. Commun. **2:** 178–184.

Chumley, F.G., and Valent, B. (1990). Genetic analysis of melanin-deficient, nonpathogenic mutants of *Magnaporthe grisea*. Mol. Plant Microbe Interact. **3:** 135–143.

Couch, B.C., and Kohn, L.M. (2002). A multilocus gene genealogy concordant with host preference indicates segregation of a new species, *Magnaporthe oryzae*, from *M. grisea*. Mycologia **94:** 683–693.

Dean, R.A. (1997). Signal pathways and appressorium morphogenesis. Annu. Rev. Phytopathol. **35:** 211–234.

de Jong, J.C., McCormack, B.J., Smirnoff, N., and Talbot, N.J. (1997). Glycerol generates turgor in rice blast. Nature **389:** 471–483.

Douglas, L.M., Alvarez, F.J., McCreary, C., and Konopka, J.B. (2005). Septin function in yeast model systems and pathogenic fungi. Eukaryot. Cell **7:** 1503–1512.

Fankhauser, C., and Simanis, V. (1994). The *cdc7* protein kinase is a

dosage dependent regulator of septum formation in fission yeast. EMBO J. **13:** 3011–3019.

Gladfelter, A., and Berman, J. (2009). Dancing genomes: Fungal nuclear positioning. Nat. Rev. Microbiol. **7:** 875–886.

Gladfelter, A.S., Hungerbuehler, A.K., and Phillipsen, P. (2006). Asynchronous nuclear division cycles in multinucleated cells. J. Cell Biol. **172:** 347–362.

Gladfelter, A.S., Kozubowski, L., Zyla, T.R., and Lew, D.J. (2005). Interplay between septin organization, cell cycle and cell shape in yeast. J. Cell Sci. **118:** 1617–1628.

Gonzalez-Novo, A., Labrador, L., Jimenez, A., Sanchez-Perez, M., and Jimenez, J. (2006). Role of septin Cdc10 in the virulence of *Candida albicans*. Microbiol. Immunol. **50:** 499–511.

Hamer, J.E., Howard, R.J., Chumley, F.G., and Valent, B. (1988). A mechanism for surface attachment in spores of a plant pathogenic fungus. Science **239:** 288–290.

Harris, S.D. (2001). Septum formation in *Aspergillus nidulans.* Curr. Opin. Microbiol. **4:** 736–739.

Kaminskyj, S.G.W. (2000). Septum position is marked at the tip of *Aspergillus nidulans* hyphae. Fungal Genet. Biol. **31:** 105–113.

Kershaw, M.J., and Talbot, N.J. (2009). Genome-wide functional analysis reveals that infection-assciated fungal autophagy is essential for rice blast disease. Proc. Natl. Acad. Sci. USA **106:** 15967–15972.

Koning, A.J., Lum, P.Y., Williams, J.M., and Wright, R. (1993). $DiOC_6$ staining reveals organelle structure and dynamics in living yeast cells. Cell Motil. Cytoskeleton **25:** 111–128.

Kozubowski, L., and Heitman, J. (2010). Septins enforce morphogenetic events during sexual reproduction and contribute to virulence of *Cryptococcus neoformans.* Mol. Microbiol. **75:** 658–675.

Leung, H., Borromeo, E.S., Bernardo, M.A., and Notteghem, J.L. (1988). Genetic analysis of virulence in the rice blast fungus *Magnaporthe grisea.* Genetics **78:** 1227–1233.

Lew, D.J. (2003). The morphogenesis checkpoint: How yeast cells watch their figures. Curr. Opin. Cell Biol. **15:** 648–653.

Lindsey, R., Cowden, S., Hernandez-Rodriguez, Y., and Momany, M. (2010). Septins AspA and AspC are important for normal development and limit the emergence of new growth foci in the multicellular fungus *Aspergillus nidulans.* Eukaryot. Cell **9:** 155–163.

Mitchell, T.K., and Dean, R.A. (1995). The cAMP-dependent protein kinase catalytic subunit is required for appressorium formation and pathogenesis by the rice blast pathogen *Magnaporthe grisea.* Plant Cell **7:** 1869–1878.

Oldenburg, K.R., Vo, K.T., Michaelis, S., and Paddon, C. (1997). Recombination-mediated PCR-directed plasmid construction in vivo in yeast. Nucleic Acids Res. **25:** 451–452.

Oliferenko, S., Chew, T.G., and Balasubramanian, M.K. (2009). Positioning cytokinesis. Genes Dev. **23:** 660–674.

Park, G., Xue, C., Zheng, L., Lam, S., and Xu, J. (2002). *MST12* regulates infectious growth but not appressorium formation in the rice blast fungus *Magnaporthe grisea.* Mol. Plant Microbe Interact. **15:** 183–192.

Park, H.O., Bi, E., Pringle, J.R., and Herskowitz, I. (1997). Two active states of the Ras-related Bud1/Rsr1 protein bind to different effectors to determine yeast polarity. Proc. Natl. Acad. Sci. USA **94:** 4463–4468.

Pearson, C.L., Xu, K., Sharpless, K.E., and Harris, S.D. (2004). MesA, a novel fungal protein required for the stabilisation of polarity axes in *Aspergillus nidulans.* Mol. Biol. Cell **15:** 3658–3672.

Saunders, D.G.O., Aves, S.J., and Talbot, N.J. (2010). Cell cycle-mediated regulation of plant infection by the rice blast fungus *Magnaporthe oryzae*. Plant Cell **22:** 497–507.

Schuyler, S.C., and Pellman, D. (2001). Search, capture and signal: Games microtubules and centrosomes play. J. Cell Sci. **114:** 247–255.

Straube, A., Weber, I., and Steinberg, G. (2005). A novel mechanism of nuclear envelope break-down in a fungus: Nuclear migration strips off the envelope. EMBO J. **24:** 1674–1685.

Sweigard, J.A., Carroll, A.M., Farrall, L., and Valent, B. (1997). A series of vectors for fungal transformation. Fungal Genet. Newsl. **44:** 52–53.

Talbot, N.J., Ebbole, D.J., and Hamer, J.E. (1993). Identification and characterization of *MPG1*, a gene involved in pathogenicity from the rice blast fungus *Magnaporthe grisea.* Plant Cell **5:** 1575–1590.

Thines, E., Weber, R.W.S., and Talbot, N.J. (2000). MAP kinase and protein kinase A-dependent mobilisation of triacylglycerol and glycogen during appressorium turgor generation by *Magnaporthe grisea.* Plant Cell **12:** 1703–1718.

Tucker, S.L., and Talbot, N.J. (2001). Surface attachment and pre-penetration stage development by plant pathogenic fungi. Annu. Rev. Phytopathol. **39:** 385–417.

Tucker, S.L., Thornton, C.R., Tasker, K., Jacob, C., Giles, G., Egan, M., and Talbot, N.J. (2004). A fungal metallothionein is required for pathogenicity of *Magnaporthe grisea*. Plant Cell **16:** 1575–1588.

Ukil, L., De Souza, C.P., Lui, H.L., and Osmani, S.A. (2009). Nucleolar separation from chromosomes during *Aspergillus nidulans* mitosis can occur without spindle forces. Mol. Biol. Cell **20:** 2132–2145.

Veneault-Fourrey, C., Barooah, M., Egan, M., Wakley, G., and Talbot, N.J. (2006). Cell cycle-regulated autophagic cell death is necessary for plant infection by the rice blast fungus. Science **312:** 580–583.

Wang, Z., Thornton, C.R., Kershaw, M.J., Debao, L., and Talbot, N.J. (2003). The glyoxylate cycle is required for temporal regulation of virulence by the plant pathogenic fungus *Magnaporthe grisea.* Mol. Microbiol. **47:** 1601–1612.

Westfall, P.J., and Momany, M. (2002). *Aspergillus nidulans* septin AspB plays pre- and postmitotic roles in septum, branch, and conidiophore development. Mol. Biol. Cell **13:** 110–118.

Wilson, R.A., and Talbot, N.J. (2009). Under pressure: Investigating the biology of plant infection by *Magnaporthe oryzae.* Nat. Rev. Microbiol. **7:** 185–195.

Wolkow, T.D., Harris, S.D., and Hamer, J.E. (1996). Cytokinesis in *Aspergillus nidulans* is controlled by cell size, nuclear positioning and mitosis. J. Cell Sci. **109:** 2179–2188.

Xu, J.R., and Hamer, J.E. (1996). MAP kinase and cAMP signaling regulate infection structure formation and pathogenic growth in the rice blast fungus *Magnaporthe grisea.* Genes Dev. **10:** 2696–2706.

Xu, J.R., Urban, M., Sweigard, J.A., and Hamer, J.E. (1997). The *CPKA* gene of *Magnaporthe grisea* is essential for appressorial penetration. Mol. Plant Microbe Interact. **10:** 187–194.

Yeh, E., Yang, C., Chin, E., Maddox, P., Salmon, E.D., Lew, D.J., and Bloom, K. (2000). Dynamic positioning of mitotic spindles in yeast: Role of microtubule motors and cortical determinants. Mol. Biol. Cell **11:** 3949–3961.